

LETTER TO THE EDITOR

Absolute cross section for the formation of N_2^+ ($X^2\Sigma_g^+$) ions produced by electron impact on N_2 N Abramzon^{†‡}, R B Siegel^{†§} and K Becker[‡][†] Department of Physics, City College of CUNY, New York, NY 10031, USA[‡] Department of Physics and Engineering Physics, Stevens Institute of Technology, Hoboken, NJ 07030, USA

Received 11 March 1999, in final form 13 April 1999

Abstract. A combination of electron scattering and laser-induced fluorescence (LIF) techniques has been employed in an absolute experimental determination of the N_2^+ ($X^2\Sigma_g^+$) ionization cross section as a function of electron energy from threshold to 200 eV. N_2^+ ground-state ions, resulting from electron impact on N_2 , are detected by laser-induced fluorescence of the N_2^+ $X^2\Sigma_g^+ \rightarrow B^2\Sigma_u^+$ transition at 391 nm. The relative ionization cross section obtained from LIF spectra taken at different electron energies is put on an absolute scale by calibration relative to the well known electron-impact cross section for the formation of helium atoms in the 2^3S state from the 1^1S ground state. The He 2^3S atoms are probed via LIF of the $2^3S \rightarrow 3^3P$ transition at 389 nm in the same apparatus using the same detection equipment and laser-induced fluorescence technique at essentially the same wavelength that is used in the measurement of the N_2^+ (X) cross section. The cross section peaks at 60 eV with a maximum value of $80 \times 10^{-18} \text{ cm}^2$. At 100 eV, our cross section value is $(74.9 \pm 7.5) \times 10^{-18} \text{ cm}^2$, which is in good agreement with the value of $(86.9 \pm 7.0) \times 10^{-18} \text{ cm}^2$ reported by Doering and Yang (1996 *J. Geophys. Res.* **102** 9683) who used a different experimental technique.

The ionization of molecules by electron impact is an important process in plasmas, gas discharges, planetary, stellar and cometary atmospheres, aeronomy, radiation chemistry and mass spectrometry [1, 2]. The formation of molecular parent ions by electron impact is generally dominated by processes leading to ions in the electronic ground state [1–3]. Molecular nitrogen (N_2) and oxygen (O_2) are among the few molecules which have significant probabilities that the electron-impact ionization leads to electronically excited parent ions [4–7]. Three electronic states of N_2^+ are populated appreciably following electron-impact ionization of N_2 , the $X^2\Sigma_g^+$ ground state and the $A^2\Pi_u$ and $B^2\Sigma_u^+$ excited states. The cross section for the ionization excitation of N_2 to the N_2^+ B-state is rather well known from various experiments (see [5] for a summary). The total N_2 ionization cross section [8] and the total N_2^+ parent ionization cross section [9–12] are also well known from experiment to better than 10%. On the other hand, the experimentally determined cross section for the formation of N_2^+ ions in the A-state is known only to within about 50%, which can be attributed to the long radiative lifetime of the state [13–15]. This renders it impossible to estimate the cross section for the formation of N_2^+ ($X^2\Sigma_g^+$) ground-state ions from other available N_2 ionization cross sections with reasonable confidence.

§ Present address: National Institute of Standards and Technology (NIST), Gaithersburg, MD 20899, USA.

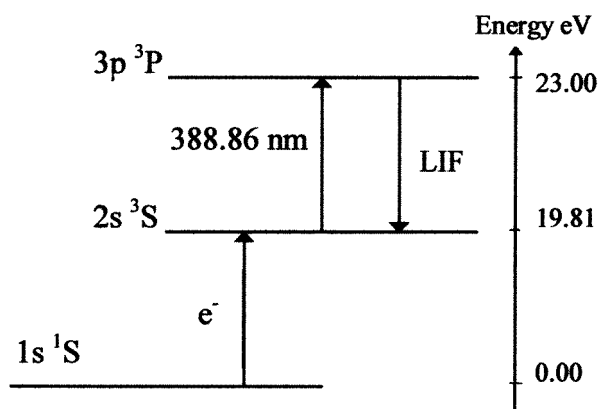


Figure 1. Partial energy level diagram of helium after Bashkin and Stoner [21] showing those energy levels that are pertinent to the present work. The electron-impact excitation route is labelled by ' e^- ' and the LIF route is labelled by 'LIF'.

Doering and co-workers used the electron–electron coincidence ($e, 2e$) technique in a direct experimental measurement of electron-impact ionization–excitation branching ratios in N_2 and O_2 [4–7] at a single electron energy of 100 eV. In the case of N_2 , their branching ratios, in conjunction with the known total parent N_2^+ ionization cross section, allowed the extraction of absolute state-selected ionization cross sections at 100 eV. Their cross section values of $86.9 \times 10^{-18} \text{ cm}^2$ (X-state), $87.9 \times 10^{-18} \text{ cm}^2$ (A-state) and $19.2 \times 10^{-18} \text{ cm}^2$ (B-state), with quoted error margins of less than 10% [6] are in poor agreement with those extracted by Van Zyl and Pendleton [4] from the critical analysis of all previously reported cross sections, $60.5 \times 10^{-18} \text{ cm}^2$ (X-state, 45% uncertainty), $101.0 \times 10^{-18} \text{ cm}^2$ (A-state, 19% uncertainty) and $27.4 \times 10^{-18} \text{ cm}^2$ (B-state, 10% uncertainty) at 100 eV. One might argue that the cross sections of Doering and Yang [6] are more reliable, since they are based on the result of new experimental data. However, acceptance of the cross sections of Doering and Yang [6] requires the value of the previously accepted N_2^+ B-state ‘benchmark’ cross section of Borst and Zipf [16] to be lowered by about 30%, which exceeds the stated uncertainty of that cross section significantly.

Recently, we determined the relative $N_2^+(X \ ^2\Sigma_g^+)$ ionization cross section as a function of electron energy using a combination of electron scattering and laser-induced fluorescence (LIF) techniques [17]. $N_2^+(X)$ ions produced by electron impact on ground-state N_2 were probed by laser-induced fluorescence of the $N_2^2 \ X \ ^2\Sigma_g^+ \rightarrow B \ ^2\Sigma_u^+$ transition at 391 nm with a tunable dye laser. LIF spectra obtained at different electron energies yielded the relative $N_2^+(X)$ cross section, which was put on an absolute scale by normalization to the absolute cross section value of Doering and Yang [6] at 100 eV. In light of the above discussion, we have decided to employ a different absolute calibration procedure for our relative $N_2^+(X)$ cross section which relies on the well known electron-impact cross section for formation of He $2 \ ^3S$ atoms from the $1 \ ^1S$ ground state [18–20]. The He $2 \ ^3S$ atoms are probed by LIF of the $2 \ ^3S \rightarrow 3 \ ^3P$ transition at 389 nm using data obtained in the same apparatus employing the same experimental set-up and LIF technique at essentially the same wavelength and the same detection equipment that is used in the determination of the $N_2^+(X)$ cross section. A partial energy level diagram of He, indicating the relevant energy levels [21], is shown in figure 1.

The experimental arrangement and data acquisition and analysis procedures employed in the experimental determination of the relative $N_2^+(X)$ cross section have been described in detail

in a previous publication [17]. The apparatus consists of an electron beam and a gas beam, intersecting at right angles inside a vacuum chamber in conjunction with a tunable laser beam, which propagates either parallel or antiparallel to the electron beam in order to maximize the overlap of the three beams. Optical detection of the LIF signal from the interaction region is made perpendicular to both the electron beam and the gas beam. The energy of the electron beam can be varied between 5 and 400 eV with typical beam currents of $3 \mu\text{A}$ at 25 eV and $20 \mu\text{A}$ at 100 eV and an energy resolution of about 0.5 eV (FWHM). The electron beam is collected in a Faraday cup which consists of three electrically insulated elements, which enables one to measure the beam current as well as the beam divergence. The gas beam is an effusive beam emanating from a multi-capillary array of rectangular shape which is positioned about 8 mm above the electron-beam axis. Roughly 50% of the total gas throughput passes through a rectangle of the size of the nozzle array in the interaction region. The pushing pressure behind the nozzle is continuously monitored by a capacitance manometer. The laser system consists of a pulsed Lumonics EX-520 excimer laser, operating at 308 nm (XeCl), which is used to pump a Lumonics HD-500 dye laser, using Exalite 392A as the dye of choice in the wavelength region under study. The laser system produces 0.0015 nm wide pulses of less than 10 ns duration of up to 3 mJ energy per pulse in the wavelength range from 375 to 397 nm. The laser beam enters and exits the vacuum chamber through Brewster-angle windows, and the beam intensity passing through the vacuum chamber is monitored by a laser pulse energy meter. The fluorescence from the interaction region is imaged onto the cathode of a thermoelectrically cooled Hamamatsu R1104 photomultiplier tube (PMT). Spectral isolation is achieved by a narrow-band interference filter. Great care was exercised to minimize the amount of scattered laser light reaching the PMT by coating all elements inside the vacuum chamber in the path of the laser beam with Aerodag-G and placing light baffles along the path of the laser beam and along the optical detection system. The output pulses of the PMT are processed by a gated photon counter whose output, in turn, is directed into a personal computer for data storage and further analysis.

We first measured the well known $\text{N}_2^+ \text{B} \rightarrow \text{X}$ and the $\text{He } 3^3\text{P} \rightarrow 2^3\text{S}$ photoemission cross sections produced directly by the continuous electron beam as a function of electron energy without laser beam in order (a) to demonstrate the proper performance of the apparatus and (b) to calibrate the energy scale of the electron beam, which was set relative to the 23.0 eV onset of the $\text{He } 3^3\text{P} \rightarrow 2^3\text{S}$ photoemission cross section [21]. With the laser beam present, a suitable delay after the end of the laser pulse was introduced (100 ns in the case of He and 55 ns in the case of N_2) before the LIF signal was recorded, to ensure that the scattered laser light reaching the PMT had decayed to a level where it no longer swamped the LIF signal. The LIF calibration measurements in N_2 were carried out at 100 eV where the $\text{N}_2^+(\text{X})$ cross section is near to its maximum. In He, we chose an electron beam energy of 20.4 eV, which was motivated by several factors: (a) the $1^1\text{S} \rightarrow 2^3\text{S}$ excitation cross section is sufficiently large at this energy [18–20] to produce an appreciable density of He 2^3S atoms; (b) this energy is just below the 20.61 eV onset for the formation of metastable He 2^1S atoms [21], which is important in view of the fact that the most reliable absolute cross section values are available only for the formation of the unresolved He $2^{1,3}\text{S}$ metastable states from the 1^1S ground state; and (c) the energy of 20.4 eV is below the threshold for populating the helium 3^3P state, the lowest-lying state above the 2^3S state which can decay radiatively to the 2^3S state, so that the LIF measurement in He is free of any $3^3\text{P} \rightarrow 2^3\text{S}$ background arising from the direct population of the upper state from the He ground state by the continuous electron beam. The LIF measurements were carried out as described previously [17]. After the end of the laser pulse, and after the above-mentioned suitable delay had elapsed, a first gate (gate A) was opened for a period T , corresponding to about

five times the radiative lifetime of the radiating state. The data in gate A contain the LIF signal, any residual background and/or noise, and, in the case of N_2^+ , also the $N_2^+ B \rightarrow X$ fluorescence produced by the continuous electron beam. At time T , gate A was closed and a second gate (gate B) was opened for the same period T . Since after a period of five lifetimes any residual LIF signal is negligible, the data in gate B contain only any residual background/noise and any N_2 fluorescence produced by the continuous electron beam. The LIF signal was then obtained as the difference between the accumulated counts in gates A and B.

LIF calibration spectra were recorded for the spectrally isolated P(6) rotational line of the $N_2 + X \rightarrow B(0, 0)$ vibrational band at 391.315 nm at an impact energy of 100 eV, and for the He $2^3S \rightarrow 3^3P$ transition at 388.86 nm at an impact energy of 20.4 eV. Figure 2(a) shows the LIF spectrum of the rotationally resolved $N_2^+(X)$ (0, 0) vibrational band near the head of the P-branch between 391.3 and 391.45 nm obtained at 100 eV, which includes the P(6) rotational line and the LIF spectrum of the He $2^3S \rightarrow 3^3P$ transition at 388.86 nm (figure 2(b)). The LIF spectra were obtained under well characterized and well controlled experimental conditions (electron beam current, target gas density, laser power, etc). The measured integrated LIF intensities (i.e. the areas under the respective LIF peaks) were normalized to the electron-beam current, the target gas density (as measured by the pushing pressure behind the gas nozzle) and the laser power. For both gases, the electron-beam currents and laser powers used were in a regime where the recorded signals varied linearly with these parameters. The pushing pressures, on the other hand, were higher than the limits at which molecular gas flow conditions through the nozzle array exist, i.e. the recorded signals did not vary linearly with the pushing pressures (gas densities). Consequently, the normalization to the target gas density had to employ a variant of the relative flow technique [22–24], which had been used successfully before in our laboratory for the normalization of optical emission signals to gas target densities outside the molecular flow regime. The procedure involves establishing intensity versus pressure curves for both gases to high statistical accuracy covering both the linear low-pressure regime, where molecular gas flow conditions exist, and the nonlinear regime of higher pressures, where the intensity increases more than linearly with pressure due to deviations from the molecular flow conditions. The deviations from linearity are quantified separately for both gases and are taken into account in the normalization procedure as described by Roque *et al* [22]. We also corrected the measured LIF spectra for a slight variation in the optical transmission of the interference filter between 388.9 and 391.3 nm [25]. We further took into account the Franck–Condon factor for the $N_2(X, \nu = 0) \rightarrow N_2^+(X, \nu = 0)$ transition of 0.917 [26]. We then accounted for the Hönl–London factor of 0.1095 [27] of the $N_2^+(X, \nu = 0 \rightarrow B, \nu = 0)$ P(6) line, and we considered the branching ratio of the $N_2^+(B, \nu = 0 \rightarrow X, \nu = 0)$ transition of 0.71 [26]. Finally, we corrected the recorded LIF intensities for the different absorption coefficients, which are proportional to the transition probabilities of the He line [28] and the N_2^+ band [29], respectively. The ratio of the ‘normalized’ LIF signals for N_2^+ and He can now be equated with the ratio of the cross sections for the formation of $N_2^+(X)$ from ground-state N_2 at 100 eV and He(2^3S) from ground-state He at 20.4 eV. Since the cross section for the He $1^1S \rightarrow 2^3S$ transition is well known [18–20], its value of $4.0 \times 10^{-18} \text{ cm}^2$ at 20.4 eV can be used to obtain the $N_2^+(X)$ cross section in a straightforward fashion. We find a value of $74.9 \times 10^{-18} \text{ cm}^2$ at 100 eV. We note that the He $1^1S \rightarrow 2^3S$ cross section varies very rapidly as a function of electron energy (compared to the 0.5 eV FWHM energy spread of our electron beam) around 20.4 eV [20]. However, the actual cross section shape between the threshold at 19.81 and about 22 eV is essentially linear [20, 30], so that the ‘effective’ cross section at 20.4 eV (i.e. the convolution of the cross section shape in this energy region with the profile of an electron beam corresponding to a peak energy of 20.4 eV and a FWHM

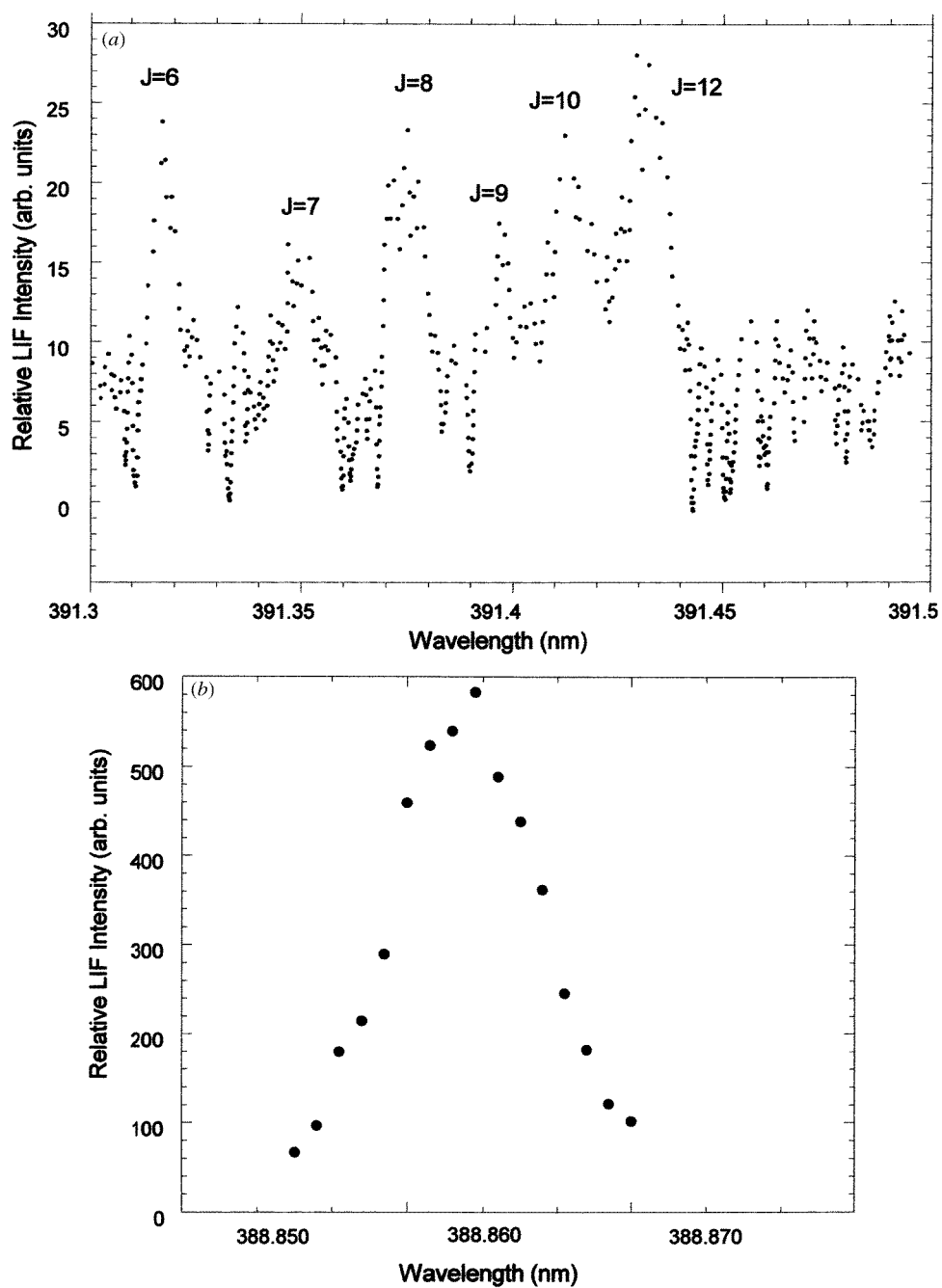


Figure 2. (a) Rotationally resolved LIF spectrum of the $N_2^+ X^2\Sigma_g^+ \rightarrow B^2\Sigma_u^+(0,0)$ vibrational band near the head of the P-branch between 391.3 and 391.45 nm obtained at an electron energy of 100 eV. The P(6) rotational line was used for calibration purposes; (b) LIF spectrum of the He $2^3S \rightarrow 3^3P$ transition at 388.86 nm at an impact energy of 20.4 eV.

energy spread of 0.5 eV) is essentially identical to the nominal cross section at 20.4 eV of $4.0 \times 10^{-18} \text{ cm}^2$ [19, 20].

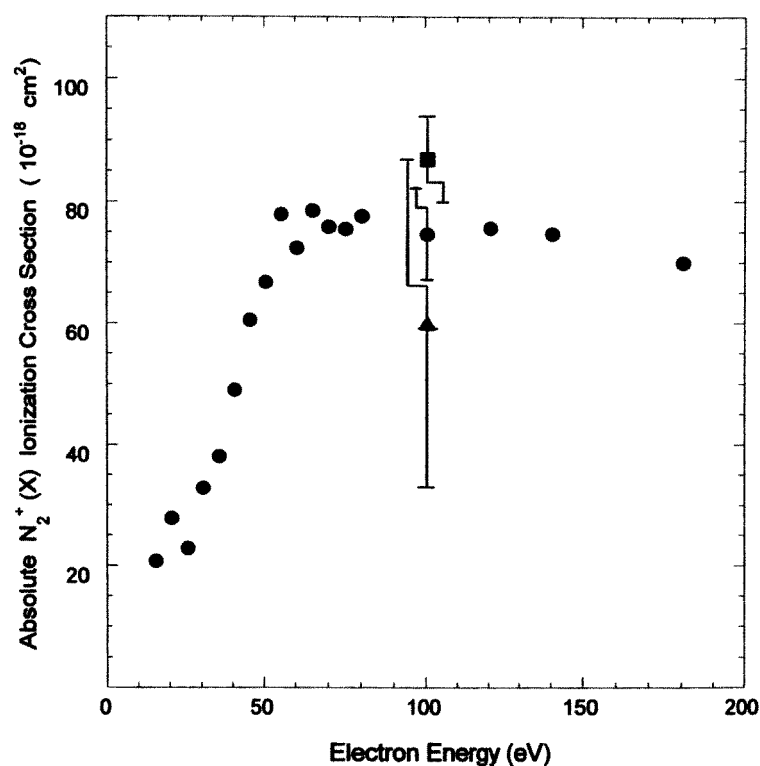


Figure 3. Absolute $N_2^+(X)$ ionization cross section in the energy range from threshold to 200 eV as a function of electron energy (full circles). Our error bar at 100 eV includes all statistical and systematic errors (see text for details). Also shown at 100 eV, are the absolute cross section value reported by Doering and Yang [6] (full square, with error bar) and by Van Zyl and Pendleton [4] (full triangle, with error bar).

The error margin of our absolute cross section is determined by the error margin in the ratio of the two LIF measurements and the inherent error in the He benchmark cross section. In our previous paper [17], we quoted a total (systematic and statistical) uncertainty of 8% in the relative $N_2^+(X)$ cross section obtained from the LIF measurements. In the present case, where the counting statistics are somewhat better and where some systematic errors cancel, we assign an error margin of 7% to the ratio of the two LIF measurements. This error margin includes the uncertainties associated with the measurement of the pushing pressure for both gases. Uncertainties in the transition probabilities, branching ratios and Franck–Condon factors are negligible [26–29] compared to the other systematic uncertainties. Mason and Newell [20] assigned an error margin of about 2.5% to the He 2^3S cross section. This results in a total error margin of our cross section of about 10%. We note that the various absolute measurements of the He $1^1S \rightarrow 2^3S$ cross section in the literature (a summary can be found in [18, 20]) carry individual error margins from 15% to 30%. However, there is excellent agreement between the various absolute measurements, which were obtained from different experimental techniques (including optical as well as non-optical methods). On that basis, Mason and Newell [20] argued that the level of confidence with which this cross section is known is much higher than the error margins of the individual measurements and assigned a 2.5% error margin to this cross section. This notion was supported in the recent review of Lin and Anderson [18]. The

absolute calibration of our $N_2^+(X)$ cross section was carried out at an electron energy of 100 eV which is sufficiently high, so that rotational warming effects, as described, for example, by Zetner *et al* [31] do not affect the calibration. The consequences of rotational warming of the N_2^+ ground-state ions in the ionization process on the relative cross section measurement are negligible when a room temperature gas beam is used [17, 32].

Figure 3 shows our absolute cross section for the formation of $N_2^+(X)$ ground-state ions as a function of electron energy from threshold to 200 eV. The cross section peaks around 60 eV with a maximum value of close to $80 \times 10^{-18} \text{ cm}^2$ and has a value of $(74.9 \pm 7.5) \times 10^{-18} \text{ cm}^2$ at 100 eV. Also shown in figure 3 are the only two other published absolute $N_2^+(X)$ cross section values (both obtained at a single electron energy of 100 eV). Doering and Yang [6] reported a value of $(86.9 \pm 7.0) \times 10^{-18} \text{ cm}^2$ obtained from an electron–electron coincidence measurement with an uncertainty of less than 10%. Van Zyl and Pendleton [4] reported a value of $60.5 \times 10^{-18} \text{ cm}^2$ based on the analysis of previously reported N_2^+ ionization cross section data (with a much larger uncertainty of about 45%). There is very good agreement between our cross section (at 100 eV) and the value of Doering and Yang [6] within the combined uncertainties. The cross section extracted by Van Zyl and Pendleton [4] from previously measured cross section data is smaller than both experimentally determined values, but not inconsistent with these higher experimentally determined values given the large margin of error of their cross section. The good agreement between the present cross section value and the one reported by Doering and Yang [6] supports the notion expressed by Doering and Yang [6] that, on the basis of their result, the previously accepted ‘benchmark’ cross section for the formation of N_2^+ ions in the B-state of Borst and Zipf [16] should be revised downward, but perhaps somewhat less than the 30% suggested by Doering and Yang [6].

We wish to acknowledge financial support of this work by the US National Science Foundation and by the US National Aeronautics and Space Administration. We also acknowledge helpful discussions with many colleagues during the course of this work, particularly with J W McConkey, V Tarnovsky and P Kurunczi.

References

- [1] Märk T D and Dunn G H (eds) 1985 *Electron Impact Ionization* (Vienna: Springer)
- [2] Janev R K (ed) 1995 *Atomic and Molecular Processes in Fusion Edge Plasmas* (New York: Plenum)
- [3] Tarnovsky V and Becker K 1995 *Plasma Sources Sci. Technol.* **4** 307
- [4] Van Zyl B and Pendleton W Jr 1995 *J. Geophys. Res.* **100** 23 755
- [5] Doering J P and Yang J 1996 *J. Geophys. Res.* **101** 19 723
- [6] Doering J P and Yang J 1996 *J. Geophys. Res.* **102** 9683
Doering J P and Yang J 1996 *J. Geophys. Res.* **102** 9691
- [7] Doering J P and Yang J 1996 *Phys. Rev. A* **54** 3977
- [8] Rapp D and Englander-Golden P 1965 *J. Chem. Phys.* **43** 1464
- [9] Itikawa Y, Hayashi M, Ichimura A, Onda K, Sakimoto K, Takanayagi K, Nakamura H and Takanayagi T 1986 *J. Phys. Chem. Ref. Data* **15** 985
- [10] Freund R S, Wetzel R C and Shul R J 1990 *Phys. Rev. A* **41** 5861
- [11] Krishnakumar E and Srivastava S K 1990 *J. Phys. B: At. Mol. Opt. Phys.* **23** 1893
- [12] Straub H C, Renault P, Lindsay B G, Smith K A and Stebbings R F 1996 *Phys. Rev. A* **54** 2146
- [13] Holland R F and Meier W B 1972 *J. Chem. Phys.* **56** 5229
- [14] Peterson J R and Moseley T J 1973 *J. Chem. Phys.* **58** 172
- [15] Piper L G, Green B D, Blumberg W A M and Wolnik S 1986 *J. Phys. B: At. Mol. Opt. Phys.* **19** 3327
- [16] Borst W L and Zipf E C 1970 *Phys. Rev. A* **1** 834
- [17] Abramzon N, Siegel R B and Becker K 1999 *Int. J. Mass Spectrom. Ion Process.* at press
- [18] Lin C C and Anderson L W 1991 Electron excitation of rare gas atoms *Advances in Atomic, Molecular, and Optical Physics* (New York: Academic) p 29

- [19] Borst W L 1974 *Phys. Rev. A* **9** 1195
- [20] Mason N J and Newell R R 1987 *J. Phys. B: At. Mol. Phys.* **20** 1357
- [21] Bashkin S and Stoner J O 1975 *Atomic Levels and Grotrian Diagrams* (Amsterdam: North-Holland)
- [22] Roque M B, Siegel R B, Martus K E, Tarnovsky V and Becker K 1991 *J. Chem. Phys.* **94** 341
- [23] Brinkman R T and Trajmar S 1981 *J. Phys. E: Sci. Instrum.* **14** 245
- [24] Trajmar S and Register D F 1984 *Electron-Molecule Collisions* ed I Shimamura and K Taganayagi (New York: Plenum)
- [25] Andover Corporation 1997 *Filter Data Sheet* Private communication
- [26] Gilmore F, Laher R and Espy P J 1992 *J. Phys. Chem. Ref. Data* **21** 1005
- [27] Herzberg G 1950 *Molecular Spectra and Molecular Structure* vol I *Spectra of Diatomic Molecules* (New York: Van Nostrand)
- [28] Wiese W L 1999 Private communication, to be published
See also Drake G W F 1996 *Atomic, Molecular, and Optical Physics Handbook* (New York: AIP)
- [29] Laux C O and Kruger C H 1992 *J. Quant. Spectrosc. Radiat. Transfer* **48** 9
- [30] Buckman S J, Hammond P, Read F H and King G C 1983 *J. Phys. B: At. Mol. Phys.* **16** 4039
- [31] Zetner P W, Hammond P, Westerveld W B, McConkey R L and McConkey J W 1988 *Chem. Phys.* **124** 453
- [32] Allison J, Kondow T and Zare R N 1979 *Chem. Phys. Lett.* **64** 202